Journal of Engineering Science 08(1), 2017, 95-102

JES
an international Journal

INVESTIGATION OF THE NANO-CRYSTALLIZATION PROCESS AND OPTIMIZATION OF ANNEALING TEMPERATURE FOR SOFT MAGNETIC PROPERTIES OF $(Fe_{0.95}Co_{0.05})_{73.5}Cu_1Nb_3Si_{13.5}B_9$RIBBON

Ratan K. Howlader[1], S. K. Shil[2*], H. N. Das[3], S. S. Sikder[2] and D. K. Saha[3]

[1]*Khulna Zilla School, Khulna, Bangladesh*
[2]*Department of Physics, Khulna University of Engineering and Technology, Khulna-9203, Bangladesh*
[3]*Materials Science Division, Atomic Energy Centre, Dhaka-1000, Bangladesh*
Received: 25 May 2017 Accepted: 28 June 2017

ABSTRACT

The evolution of crystallizationof FINEMET-like amorphous ribbon $(Fe_{0.95}Co_{0.05})_{73.5}Cu_1Nb_3Si_{13.5}B_9$ has been investigated by means of differential thermal analysis (DTA)and X-ray diffraction (XRD). The activation energy for crystallization is evaluated by Kissinger'splot. The influence of annealing process on soft magnetic properties of the studied samples have been investigated by using vibrating sample magnetometer (VSM). The ultra-soft magnetic properties are obtained after proper annealing.The saturation magnetization (M_s) ofnanocrystalline samples has slightly increased for annealing temperature (T_a) around the onset crystallization.

Keywords: *Activation Energy, Annealing Temperature, Grain Size, Saturation Magnetization, Magnetic Hysteresis.*

1. INTODUCTION

Magnetic materials played a prominent role in the discovery of new civilization and development of modern technology. Over the past several decades, amorphous and most recently, research interest in nanocrystalline soft magnetic alloys has dramatically increased. Soft magnetic materials face demanding requirements for high performance electronic and power distribution systems. With the reduction of size into nanometer range, the materials exhibit interesting properties including physical, chemical, magnetic and electrical properties comparing to conventional coarse grained counterparts. Soft magnetic nano structured materials have a number of potential technological applications(Kulik*et al.*, 1994; Miguel *et al.*, 2003; Jie Chen *et al.*, 2016; Yapi Liu *et al.*, 2013; Trilochan*et al.*, 2013; Partha*et al.*, 2010; Jing Zhi*et al.*, 1996; Kane *et al.*, 2000; Mondal*et al.*, 2012; Hassiak*et al.*, 2000).Nanocrystalline soft magnetic materials were first reported by Yoshizawa*et al.*, (1988) through controlled crystallization of Fe-Si-B amorphous alloys with the addition of copper (Cu) and niobium (Nb). The development of nanocrystalline Fe-Si-B-Nb-Cu alloys, commercially known as FINEMET, established a new approach to develop soft magnetic materials. The nanocrystalline state is achieved by subsequent heat treatment from their as cast amorphous precursor above the primary crystallization temperature. Excellent soft magnetic properties can be found innanocrystalline materials ofFe-Si-B amorphous ribbons containing Cu and Nb. The addition of Cu and Nb results in the formation of an ultra-fine grain structure. Cu is used as nucleating agent for the growth of nanocrystals while Nb for inhibiting their growth. Therefore, the appropriate amount of Cu and Nb are very important for controlling the crystallization behavior of FINEMET type amorphous alloys.Efforts were going on to improve the soft magnetic properties of FINEMET alloy by modifying the alloy compositions. M. Ohnuma*et al.*, (2003) reported that the substitution of Fe by Co decreases the saturation magnetostriction in FINEMET type amorphous alloys. The aim of the present research is to investigate the microstructural evolution of (FeCo)-Si-B-Nb-Cu amorphous alloys and to optimize the T_a for obtaining good soft magnetic properties.

2. EXPERIMENTAL

The amorphous ribbon with a composition$(Fe_{0.95}Co_{0.05})_{73.5}Cu_1Nb_3Si_{13.5}B_9$ was prepared from high purity Fe (99.9 %), Co (99.9%), Nb (99.9 %), Si (99.9 %), Cu (99.9 %) and B (99.9 %). The ribbons were produced in an arc furnace on a water-cooled copper hearth by a single roller melt-spinning technique under an atmosphere of pure argon at the Centre of Materials Science, National University of Hanoi, Vietnam. The wheel velocity was about 34 m/s. The ribbons were annealed in a vacuum heat treatment furnace at 625, 700, 725 and 750°C respectively for constant time 30 minutes and then cooled down to the room temperature. Crystallization phase analysis was carried out by DTA (SEIKO TG/DTA 6300). The

* Corresponding Author:sujitphy.kuet@gmail.com

activation energy for crystallization of primary and secondary phases have been calculated using Kissinger's equation (Kissenger, 1956):$E = -kT_p ln\left(\frac{\beta}{T_p^2}\right)$, where β is the heating rate, T_p is the crystallization peak temperature, E is the activation energy and k is the Boltzmann's constant.Amorphousity of the ribbon and nanocrystalline structure have been observed by XRD (Philips (PW 3040) X 'Pert PRO XRD) with Cu-$K_\alpha$radiation.Lattice parameter (a_0) were calculated using equations $2d\sin\theta = \lambda$ and $a_0 = d\sqrt{2}$, where $\lambda = 1.54178$Å for $Cu - K_\alpha$ radiation. Grain size (D_g) of all annealed samples of the alloy composition has been determined using Debye-Scherrer method.Si contents were calculated using the equation: $X = \frac{(a_0 - 2.8812)}{0.0022}$, where X is at.% Si in the nanograins. Magnetic properties such as field dependent specific magnetization and hysteresis were performed by using VSM.

2. RESULTS AND DISCUSSION

3.1. DTA of the sample

Figure 1 shows DTA profile of as-cast amorphous ribbon with a heating rate of 20°C/min in a nitrogen atmosphere. Two exothermic peaks are distinctly observed which correspond to two different crystallization events. The soft magnetic properties correspond to the primary crystallization of α-FeCo(Si) phase initiated at T_{x_1}. Secondary crystallizationcorresponds to FeCoB phase initiated at T_{x_2} which causes magnetic hardening of the nanocrystalline alloy. The peak temperatures (T_{P_1} and T_{P_2}) display exothermic peak, i.e., release of heat during the crystallization ofα-FeCo(Si) andFeCoB phases.

DTA traces of as-cast amorphous ribbons $(Fe_{0.95}Co_{0.05})_{73.5}Cu_1Nb_3Si_{13.5}B_9$with heating at the rate of 10–50°C/min at the step of 10°C with continuous heating from room temperature to 900°C are shown in the Figure 2. It is observed that the crystallization of each phase has occurred over a wide range of temperatures and the crystallization temperature range for the first phase is always wider than that of the second phase.It is also noted that the peak temperature shifted towards the higher valueand the crystallization temperature range increases with the increase of heating rate. That means it requires more heat energy for the formation of crystalline phases with increasing heating rate. The heat consumption is observed more during the primary crystallization. Since the crystallization of α-FeCo (Si) is completed before the onset of secondary crystallization, the less amount heat is released during rest of the crystallization process. From the Figure 2 it is seen that two crystallization events have taken place within a large temperature gap of around 135°C to 140°C. This is because the clustering of Cu atoms initiates the formation ofα-FeCo(Si) phase at temperature lower than the alloy without Co. That means, the role of Cu is to facilitate the formation of α-FeCo(Si) phase.

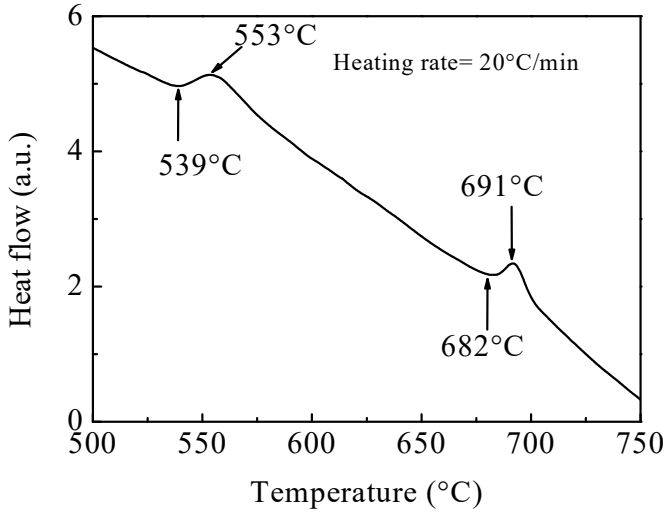

Figure 1: DTA trace of as-cast amorphous ribbon with composition $(Fe_{0.95}Co_{0.05})_{73.5}Cu_1Nb_3Si_{13.5}B_9$ for heating rate 20°C/min

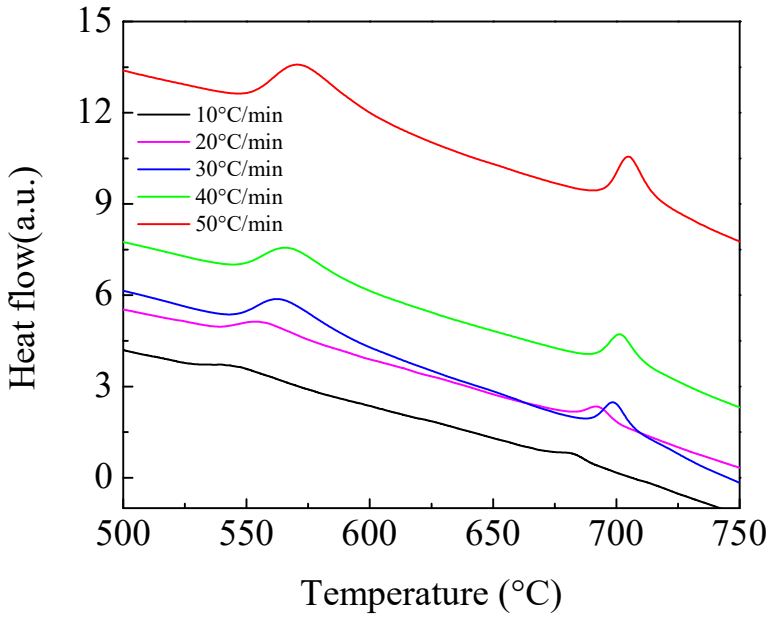

Figure 2: DTA traces of as-cast amorphous ribbon with composition $(Fe_{0.95}Co_{0.05})_{73.5}Cu_1Nb_3Si_{13.5}B_9$ for different heating rates

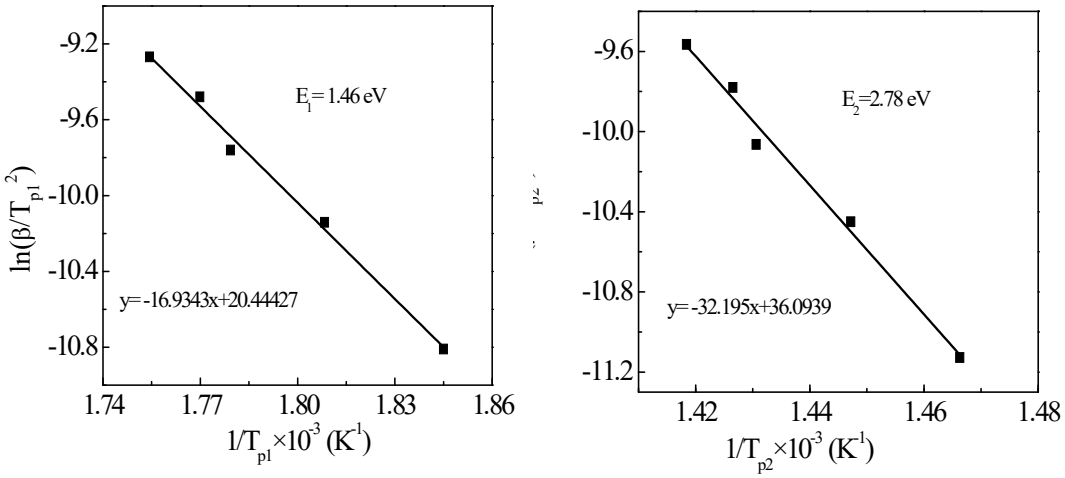

Figure 3(a,b): Kissinger's plot to determine the activation energy of α-FeCo(Si) phase and FeCoB phase

From the Figure 3(a) and Fig. 3(b) the activation energy for the α-FeCo(Si) phase and FeCoB phase is found to be E_1= 1.46 eV and E_2= 2.78 eV respectively. In the early stage of crystallization Cu clusters dominated the crystallization of α-FeCo(Si) phase and leads to a low activation energy but with the increase of crystalline volume fraction, the Cu rich regions gradually run out. Consequently, the Nb and Cu rich regions block the further growth of grains. The higher the Nb and B content the stronger the growth blocking process (Yoshizawa*et al.*, 1990). As a result, the activation energy is higher for nucleation of secondary phase. The values of crystallization onset temperature, peak temperature with respect to heating rate and activation energy are listed in the Table 1.

Table 1: The values of crystallization onset temperature, peak temperature with respect to heating rate and activation energy of the nanocrystalline amorphous ribbon with composition $(Fe_{0.95}Co_{0.05})_{73.5}Cu_1Nb_3Si_{13.5}B_9$

Heating rate (°C/min)	1st starting T_{x_1} (°C)	1st Peak T_{P_1} (°C)	2nd starting T_{x_2} (°C)	2nd Peak T_{P_2} (°C)	$(T_{P_2} - T_{P_1})$ (°C)	Activation energy	
						E_1 (eV)	E_2 (eV)
10	530	542	670	682	140	1.46	2.78
20	539	553	682	691	138		
30	543	562	687	699	137		
40	545	565	689	701	136		
50	547	570	690	705	135		

3.2. XRD

XRD spectra of as-cast and annealed at 550°C to 750°C for 30 minutes have been presented in Figure 4. One broad peak at 2θ=45° for the as-cast sample confirms the amorphous state. XRD pattern clearly indicates the formation of bcc Fe(Si) phase at T_a=550°C or above with the appearance of (110), (200) and (211) fundamental diffraction peaks. With the increasing of T_a, (110) peak becomes sharper which means the grains are growing bigger. From the Figure 4 it is also observed that just before (110) peak, another diffraction line with small peak at 2θ≈ 44° appeared for the samples annealed at 700°C to 750°C. This diffraction peak has been matched with $Fe_{23}B_6$ phase (boride phase). Therefore the boride phase for this sample has appeared along with bcc Fe(Si). Absence of boride phase in the XRD spectra is possibly due to very small volume fraction of $Fe_{23}B_6$.

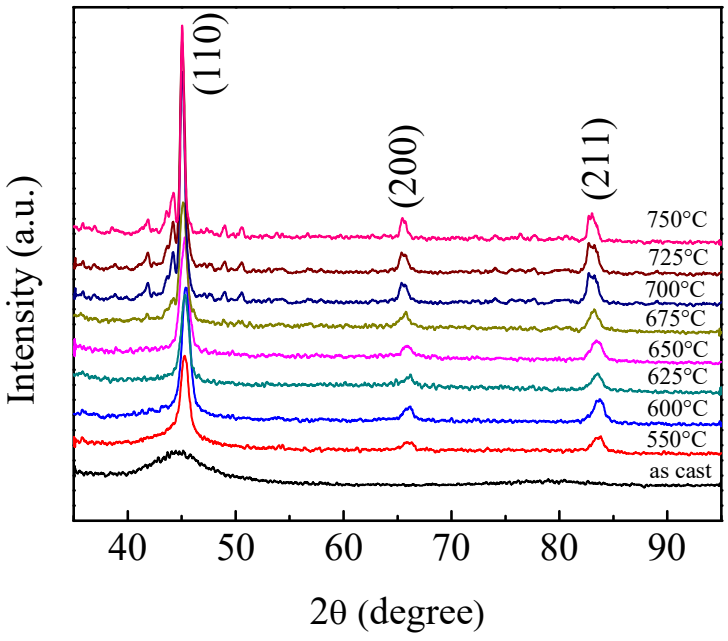

Figure 4: XRD patterns of $(Fe_{0.95}Co_{0.05})_{73.5}Cu_1Nb_3Si_{13.5}B_9$ alloy for as cast and annealed at different temperatures for 30 minutes

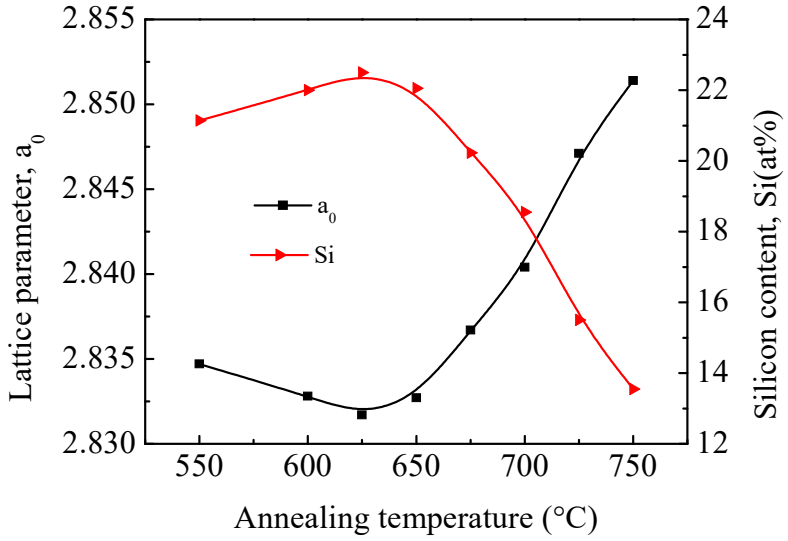

Figure 5: Variation of lattice parameter and Si-content with annealing temperature of $(Fe_{0.95}Co_{0.05})_{73.5}Cu_1Nb_3Si_{13.5}B_9$ alloy

Figure 5 shows the variation of lattice parameter (a_0) of Fe(Si) phase and Si-content with respect to the T_a of the samples. The a_0 is found to decrease with T_a up to 625°C then with further increase of T_a, a_0 increases while Si-content varies in opposite direction with T_a. This is because, with increasing T_a the diffusion of Si into α-FeCo space lattice increases and hence increases the formation of α-FeCo(Si) nanograin. At higher T_a, Si diffuses out of nanograins due to recrystallization corresponding to formation of boride phase which is consistent with the result of other FINEMET's (Franco *et al.*, 1988). Si has a smaller atomic size compared to Fe, diffuses in the α-FeCo lattice during annealing which results in a contraction of α-FeCo lattice. So the decrease of a_0 up to 625°C is expected. Since with further increase of T_a, Si diffuses out, a_0 increases.

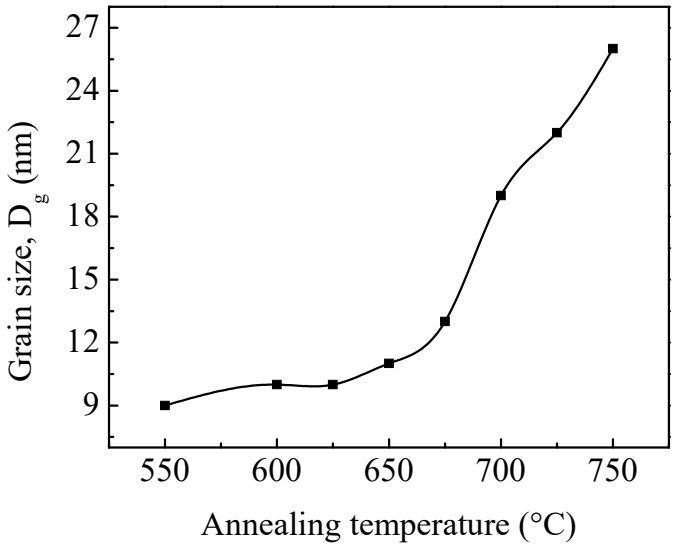

Figure 6: Variation of grain size with annealing temperature of $Fe_{0.95}Co_{0.05})_{73.5}Cu_1Nb_3Si_{13.5}B_9$ alloy

Figure 6 shows the variation of grain size (D_g) of α-Fe(Si) phase with T_a. Enhancement of D_g with T_a complies with the reported result (Mondal*et al.*, 2011). All the results of θ, d-values, FWHM, a_0, D_g and Si-content from XRD analysis are listed in Table 2.

Table2: The values of a_0, Si-content and D_g with respect to T_a of $(Fe_{0.95}Co_{0.05})_{73.5}Cu_1Nb_3Si_{13.5}B_9$ alloy

T_a (°C)	θ (degree)	D (Å)	a(Å)	FWHM	Si (at%)	D_g (nm)
550	22.6188	2.0044	2.8347	0.93	21.14	9
600	22.6343	2.0031	2.8328	0.83	22	10
625	22.6438	2.0023	2.8317	0.81	22.5	10
650	22.6355	2.0030	2.8327	0.75	22.05	11
675	22.6021	2.0058	2.8367	0.69	20.23	13
700	22.5701	2.0085	2.8404	0.45	18.55	19
725	22.5145	2.0132	2.8471	0.41	15.5	22
750	22.4791	2.0162	2.8514	0.33	13.55	26

3.3. Specific magnetization

Figure 7shows the field dependence of specific magnetization ofnanocrystalline amorphous ribbon. Maximum M_s is found for the sample annealed at 600°C. A rapid decrease in M_s has been observed for the sample annealed at 625°C. With further increase of T_a, M_s increases with increasing up to 675°C. An increase of M_s compared with amorphous state is due to the irreversible structural relaxation, changing the degree of chemical disorder of the amorphous state (Lovas*et al.*, 2000) and enhanced volume fraction of FeCo(Si) nanocrystals that are exchange coupled. It is noted that an in $M_s$due to structural relaxation has also been detected in Fe-based glasses (Berkowitz *et al.*, 1981). A rapid decrease in M_s may be connected with the enrichment of the residual amorphous phase withNb that weakens the coupling between ferromagnetic nanograins. Also the role of Si-diffusion into FeCo(Si) nanograins and the local environments may also have effect in decreasing M_s. The decrease of M_s for the sample annealed at higher temperature on ordering of Fe_3Si nanograin cannot be ruled out.

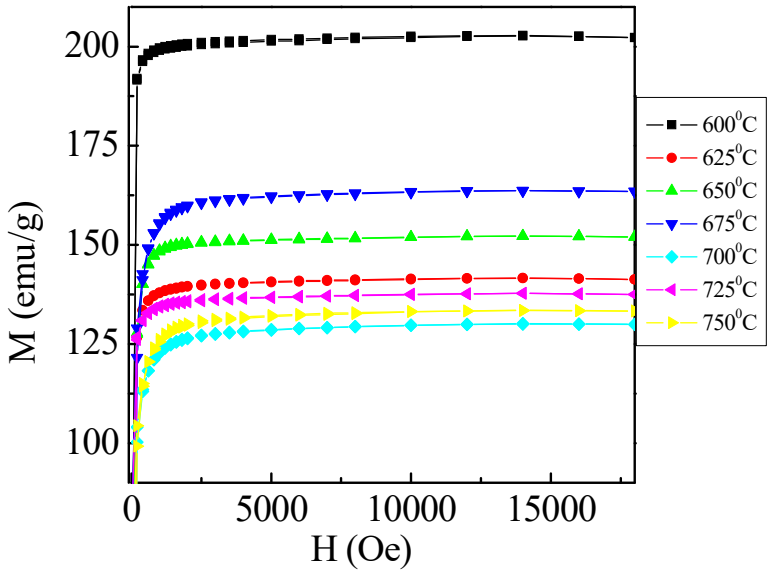

Figure 7: Specific magnetization versus magnetic field of nanocrystalline amorphous $(Fe_{0.95}Co_{0.05})_{73.5}Cu_1Nb_3Si_{13.5}B_9$ alloy for different annealing temperatures

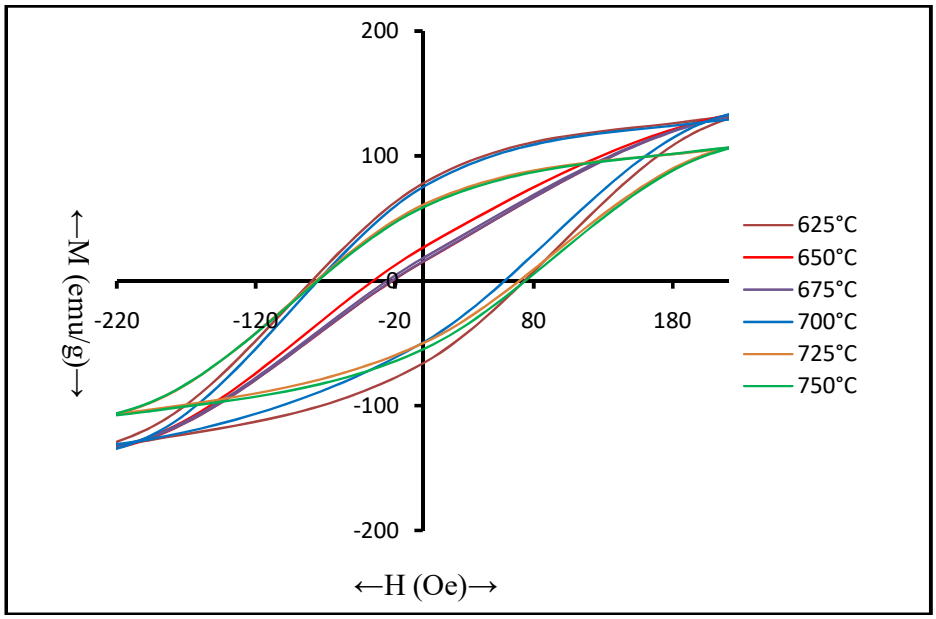

Figure 8: Magnetic hysteresis of $(Fe_{0.95}Co_{0.05})_{73.5}Cu_1Nb_3Si_{13.5}B_9$ alloy for different annealing temperatures

Figure 8 represents the hysteresis loops of all the samples at room temperature. The values of M_s, remnance induction (B_r) and coercive force (H_c) are listed in Table-3. It is observed that both B_r and H_c decrease with increasing T_a i.e., with increasing T_a the sample shifts toward soft magnetic performance.

Table3: The values of M_s, B_r and H_c of $(Fe_{0.95}Co_{0.05})_{73.5}Cu_1Nb_3Si_{13.5}B_9$ alloy for different annealing temperatures

T_a (°C)	M_s (emu/g)	B_r (emu/g)	H_c (Oe)
600	202	…	…
625	141	79	80
650	152	…	…
675	164	…	…
700	130	76	78
725	137	62	75
750	133	59	74

4. CONCLUSIONS

Nanocrystalline amorphous ribbon of the FINEMET family with a nominal composition $(Fe_{0.95}Co_{0.05})_{73.5}Cu_1Nb_3Si_{13.5}B_9$ has been studied. From this research the following conclusion can be drawn:

i. DTA reveals the primary and secondary crystallization onset temperatures with the manifestation of two well-defined peaks corresponding to nanocrystallineFeCo(Si) andFeB/FeCoB phases respectively.The knowledge of crystallization temperatures has been fruitfully utilized during the isothermal annealing of these amorphous ribbons for nanocrystallization, this ultimately controls the magnetic properties of the FINEMET alloys. The activation energy of the first and second peaks are 1.46 eV and 2.78 eV respectively. The temperature difference between two crystallization peaks is found to exist around 138°C. This peaks separation temperature is important because it denotes the crystallization stability of primary phase against detrimental boride phases which is very necessary for fabrication of high quality inductors.

ii. The amorphous state of the as-cast amorphous ribbons has been confirmed by XRD. The evolution of nanocrystallites of α-FeCo(Si) with T_a have been confirmed from the fundamental diffraction peaks. The grain size of the sample was found from 9 to 26 nm for T_a from 550 to

750°C. The crystallization onset temperature is found between 530 to 550°C which coincides well with the value obtained from DTA. The a_0 and Si content show an inverse relationship with T_a.

iii. The M_s for the sample has slightly increased withT_a around the onset crystallization whereas when annealed at higher than that, the M_s decreases again.With increasing T_a the sample shifts toward soft magnetic performance.

ACKNOWLEDGEMENTS

We are gratefulto Bangladesh Council for Scientific and Industrial Research (BCSIR) and Materials Science Division, Atomic Energy Centre, Dhaka (AECD) for giving experimental facilities and cordial co-operations.

REFERENCES

Kulik, T., Hernando, A. and Vasquez, M.,"Correlation between structure and the magnetic properties of amorphous and nanocrystalline $Fe_{73.5}Cu_1Nb_3Si_{22.5-x}B_x$ alloys", J. Magn. Magn. Mater, (1994), Vol.133, pp.310-313.

Miguel, C.,Zhuov, A. P. and Gonzalez, J., "Magnetoimpedance of stress and/ or field annealed $Fe_{73.5}Cu_1Nb_3Si_{15.5}B_7$ amorphous and nanocrystalline ribbon", J. Magn. Magn. Mater, (2003), Vol.254-255,pp. 463-465.

Jie Chen and Zhenghou Zhu,"The study on surface chemical modification of $Fe_{71.5}Cu_1Nb_3Si_{13.5}B_9V_2$ amorphous alloy ribbons and its piezomagnetic effect", J. Magn. Magn. Mater, (2016), Vol. 419,pp. 451-455.

Yapi Liu, Yide Yi, Wei Shao and Yanfang Shao,"Microstructure and magnetic properties of soft magnetic cores of amorphous and nanocrystalline alloys, J. Magn. Magn. Mater,(2013), Vol. 330,pp. 119-133.

TrilochanSahoo, Mojumdar, B.,Srinivas, V.,Srinivas, M.,Nath, T. K. and Agarwal, G., "Improved magnetoimpedance and mechanical properties on nanocrystallization of amorphous $Fe_{68.5}Si_{18.5}Cu_1Nb_3B_9$ ribbons", J. Magn. Magn. Mater, (2013), Vol.343, pp. 13-20.

ParthaSarkar, Mohanta, O., Pal, S. K., Panda, A. K. and Mitra, A., "Magneto-Impedance behavior of Co-Fe-Nb-Si-B based ribbons", J. Magn. Magn. Mater, (2010), Vol.322, No. 8, pp. 1026-1031.

Jing Zhi, Kai-Yuan He, Li-Zbi Cheng and Yu-jan Fu,"Influence of the elements Si/B on the structure and magnetic properties of nanocrystalline $(Fe, Cu, Nb)_{77.5}Si_xB_{22.5-x}$ alloys", J. Magn. Magn. Mater,(1996), Vol. 153, pp. 315-319.

Kane, S. N.,Sarabhi, S.,Gupta, A.,Varga, L. K. and Kulik, T., "Effect of quenching rate on crystallization in $Fe_{73.5}Si_{13.5}B_9Cu_1Nb_3$ alloy", J. Magn. Magn. Mater, (2000), Vol.215-216,pp. 372-374.

Ghannami, M. El,Kulik, T., Hernando, A.,FermandezBarquin, L., Gomez Sal, J. C.,Gorria, P. and Barandarian, J. M., "Influence of the Preparation Condition on the Magnetic Properties and Electrical Resistivity of $Fe_{73.5}Cu_1Nb_3Si_{13.5}B_9$Nanocrystalline alloy", J. Magn. Magn. Mater,(1994), Vol. 133, pp. 314-316.

Mondal, S. P.,KaziHanium Maria, Sikder, S. S.,ShamimaChoudhury, Saha, D. K. and Hakim, M. A., "Influence of Annealing Conditions on Nanocrystalline and Ultra-Soft Magnetic Properties of $Fe_{73.5}Cu_1Nb_3Si_{13.5}B_9$ alloy", J. Mater. Sci. Technol., (2012), Vol. 28, No. 1, pp. 21-26.

Hassiak, M.,Zbroszczyk, J., Olszewki, J.,Ciuzynska, W. H.,Wyslocki, B. andBlachowicz, A., "Effect of cooling rate on magnetic properties of amorphous and nanocrystalline $Fe_{73.5}Cu_1Nb_3Si_{13.5}B_9$ alloy", J. Magn. Magn. Mater, (2000), Vol.215-216,pp. 410-412.

Yoshizawa, Y.,Oguma, S. and Yamauchi, K., "New Fe-based Soft Magnetic Alloys Composed of Ultra-fine Grains Structure", J. Appl. Phys., (1988), Vol.64,pp. 6044-6046.

Ohnuma,M., Pins, D. H., Abe, T., Onodera, H. andHono, K., "Optimazition of the microstructure and properties of Co-substituted Fe-Si-B-Nb-Cu nanocrystalline soft magnetic alloys", J. Appl. Phys., (2003), Vol. 93, No. 11, pp.1986-1994.

Kissenger, H. E., "Variation of Peak Temperature with Heating Rate in Differential Thermal Analysis", J. Res. Nat. Bur. Stand., (1956), Vol. 57,pp. 217-221.

Yoshizawa, Y. and Yamachi, K., "Fe-based soft magnetic alloys composed of ultra-fine grain structure", Mater. Trans. JIM, (1990), Vol. 31,pp. 307-314.

Franco, V.,Conde, C. F. andConde, A.,"Changes in magnetic anisotropy distribution during structural evolution of $Fe_{76}Si_{10.5}B_{9.5}Cu_1Nb_3$, J. Magn. Magn. Mater", (1998),Vol.185,pp. 353-359.

Mondal, S. P.,KaziH. M., Sikder, S. S.,Shireen A., Hakim, M. A. and Choudhury S.,"Correlation between Structure and the magnetic properties of amorphous and nanocrystalline $Fe_{74}Cu_{0.5}Nb_3Si_{13.5}B_9$ alloys", Journal of Bangladesh Academy of Sciences, (2011), Vol. 35, No. 2,pp. 187-195.

Lovas, A., Kiss, L. F. andBalong, L.,"Saturation magnetization and amorphous Curie point changes during the early stage of amorphous nanocrystalline transformation of a FINEMET type alloy", J. Magn. Magn. Mater, (2000), Vol.215-216,pp. 463-465.

Berkowitz, A. E., Walter, V. K. andWall, F.,"Magnetic Properties of Amorphous Particles Produced by Spark Erosion", Phys. Rev. Lett., (1981), Vol.46, pp. 1484-1487.